

Infrared Spectroscopy of Matrix-Isolated Polycyclic Aromatic Hydrocarbon Ions. 5. PAHs Incorporating a Cyclopentadienyl Ring[†]

D. M. Hudgins,* C. W. Bauschlicher, Jr., and L. J. Allamandola

NASA Ames Research Center, MS 245–6, Moffett Field, California 94035

J. C. Fetzer

Chevron Research Company, Richmond, California 94802

Received: November 5, 1999; In Final Form: February 9, 2000

The matrix-isolation technique has been employed to measure the mid-infrared spectra of the ions of several polycyclic aromatic hydrocarbons whose structures incorporate a cyclopentadienyl ring. These include the cations of fluoranthene (C₁₆H₁₀), benzo[*a*]fluoranthene, benzo[*b*]fluoranthene, benzo[*j*]fluoranthene, and benzo[*k*]fluoranthene (all C₂₀H₁₂ isomers), as well as the anions of benzo[*a*]fluoranthene and benzo[*j*]fluoranthene. With the exception of fluoranthene, which presented significant theoretical difficulties, the experimental data are compared to theoretically calculated values obtained using density functional theory (DFT) at the B3LYP/4-31G level. In general, there is good overall agreement between the two data sets, with the positional agreement between the experimentally measured and theoretically predicted bands somewhat better than that associated with their intensities. The results are also consistent with previous experimental studies of polycyclic aromatic hydrocarbon ions. Specifically, in both the cationic and anionic species the strongest ion bands typically cluster in the 1450 to 1300 cm⁻¹ range, reflecting an order-of-magnitude enhancement in the CC stretching and CH in-plane bending modes between 1600 and 1100 cm⁻¹ in these species. The aromatic CH out-of-plane bending modes, on the other hand, are usually modestly suppressed ($\leq 2x - 5x$) in the cations relative to those of the neutral species, with the nonadjacent CH modes most strongly affected. The ionization effect on the analogous anion modes is more varied, with both enhancements and suppressions observed. Finally, while no cation features have been observed in the 3100–2950 cm⁻¹ aromatic CH stretching region, bands arising from these modes are observed for each of the anions addressed in these studies. This agrees qualitatively with the theoretical calculations which predict that, in stark contrast to the order of magnitude suppression encountered in the cations, the total intensity in these modes is actually enhanced by about a factor of 3 in the anions relative to the neutral species. This is the first time that the CH stretching features of an isolated PAH ion have been observed experimentally.

I. Introduction

Over the past decade, evidence has been mounting supporting the idea that polycyclic aromatic hydrocarbons (PAHs) are the carriers of a very common family of interstellar infrared fluorescence bands. These emission features are observed in many galactic and extragalactic objects, indicating that the carriers are a universally important component of interstellar matter.^{1a–d} Proper testing of this model and the exploitation of PAHs as probes of the interstellar medium has been limited by the lack of spectroscopic data on PAHs under conditions relevant to the emission regions where they are isolated (i.e., gaseous) and likely to be ionized.² Motivated in no small part by this emerging interstellar importance, the past decade has seen a renaissance in experimental^{3a–e} and theoretical^{4a–f} methods for determining the infrared spectroscopic properties of PAHs under conditions relevant to the astrophysical problem. Of the experimental techniques, the matrix-isolation technique has proven particularly well suited to the study of both the cations^{3b,5a–e,6a–f} and, more recently, the anions^{7a,b} of these species. In this regard, we have undertaken an ongoing, systematic study

of the infrared spectroscopic properties of argon matrix-isolated PAHs and their ions. The ions whose spectra are reported here have been generated using the in situ photoionization methods developed by Jacox and her colleagues over the past three decades.⁸ Although the primary motivation for this research is to investigate the role of PAHs in the interstellar medium, the results are of general interest as ionized PAHs are considered to be important intermediates in combustion,^{9a–c} and many PAH intermediates and primary reaction products are carcinogenic.^{10a,b}

Previous papers in this series have focused on the infrared spectral properties of the cations of naphthalene,^{3b} the thermodynamically most favored PAH structures through coronene,^{6a} the polyacenes through pentacene,^{6b} and the tetracyclic isomers chrysene and 1,2-benzanthracene.^{6c} In this paper we continue to investigate spectral trends associated with structure, focusing on PAHs that incorporate a cyclopentadienyl ring in their framework. Specifically, we have studied the cations of fluoranthene (C₁₆H₁₀) and four isomeric benzofluoranthenes: benzo[*a*]fluoranthene (benz[*e*]aceanthrylene), benzo[*b*]fluoranthene (benz[*e*]acephenanthrylene), benzo[*j*]fluoranthene, and benzo[*k*]fluoranthene (all C₂₀H₁₂). The structures of these compounds are shown in Figure 1. In addition, we have also studied the anions of benzo[*a*]– and benzo[*j*]fluoranthene which are pro-

[†] Part of the special issue "Marilyn Jacox Festschrift".

* To whom correspondence should be addressed.

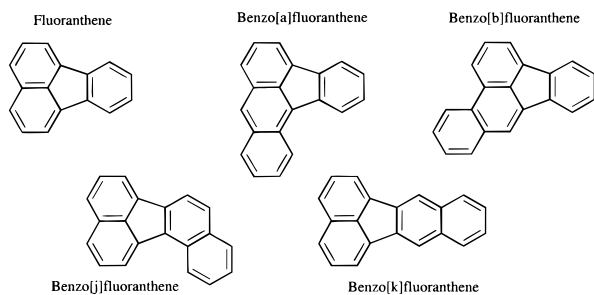


Figure 1. The structures of fluoranthene, benzo[*a*]fluoranthene, benzo[*b*]fluoranthene, benzo[*j*]fluoranthene, and benzo[*k*]fluoranthene.

duced serendipitously in the cation experiments through photoelectron attachment to residual neutral PAH molecules in the matrix. The neutral spectra of these PAHs have previously been published.^{6f}

II. Experimental and Theoretical Methods

A. Experimental Techniques. The experimental technique will be described only briefly since a detailed description of our procedure is available elsewhere.^{3b,6a} Samples are prepared by vapor co-deposition of the PAH of interest with an overabundance of argon onto a 10 K CsI window suspended in a high-vacuum chamber ($p < 10^{-8}$ mTorr). PAH samples are vaporized from heated Pyrex tubes while argon is admitted through a length of liquid nitrogen cooled copper tubing. These ports are oriented such that the two vapor streams coalesce at the surface of the cold window. Optimum deposition temperatures for the PAHs studied were as follows: fluoranthene, 57 °C; benzo[*a*]fluoranthene, 95 °C; benzo[*b*]fluoranthene, 99 °C; benzo[*j*]fluoranthene, 94 °C; and benzo[*k*]fluoranthene, 105 °C. Under these conditions an Ar/PAH ratio in excess of 1000/1 is achieved.^{6d} Once an appropriate amount of material has accumulated, an infrared spectrum of the sample is recorded. Comparison of this spectrum to that obtained after the sample is exposed to ionizing radiation permits identification of PAH ion features which appear upon photolysis.

To aid in distinguishing the bands of PAH ions from those of other, spurious photoproducts, parallel experiments are conducted in which the argon matrix is doped with an electron acceptor at a concentration of about 1 part in 1000. When necessary, these experiments are also useful for distinguishing between the cation and anion bands of a PAH since formation of the latter species is effectively quenched in the presence of an electron acceptor. While in past PAH cation studies we have relied on CCl_4 as the electron acceptor, more recently we have begun to employ NO_2 for this purpose as well. This change was directly inspired by the work of Milligan and Jacox,¹¹ who first reported the facile conversion of NO_2 to NO_2^- in alkali metal-doped argon matrices and thoroughly characterized the spectroscopy of these species. Given the favorable electron affinity ($\text{EA} = 2.4 \text{ eV}^{12}$) and large cross section for electron attachment of NO_2 and the relative simplicity of the $\text{NO}_2/\text{NO}_2^-$ spectrum, this system would seem to present an ideal electron trap to facilitate studies of matrix-isolated cations. Indeed, NO_2 has proven to be a more efficient electron acceptor than CCl_4 (as measured by the level of enhancement in the PAH cation bands), and it exhibits a less complex chemistry under photolysis. Also, neither NO_2 nor its daughter NO_2^- have any strong absorptions in the 900–600 cm^{-1} aromatic CH out-of-plane bending region, a portion of the spectrum that suffers heavy obscuration (800–740 cm^{-1}) in CCl_4 -doped matrices. The strongest band of NO_2 falls near 1600 cm^{-1} , a region of the spectrum already obscured by the bands of the omnipresent H_2O

contaminant. The NO_2^- anion does, however, exhibit a strong absorption between 1240 and 1250 cm^{-1} , a region in which PAH cation features are often observed and one which is largely free of interference in CCl_4 -doped matrices. Thus, the data obtained with each of the two electron acceptors are complementary, allowing more complete spectral coverage.

Vacuum ultraviolet photolysis of the PAH/Ar matrices is accomplished with the combined 120 nm Lyman- α /160 nm molecular hydrogen emission bands (10.1 and 7.77 eV, respectively) from a microwave powered discharge in a flowing H_2 gas mixture at a dynamic pressure of 120–150 mTorr. For CCl_4 -doped samples, a CaF_2 filter (cutoff $\lambda \approx 150 \text{ nm}$) was installed in the lamp, excluding the Ly- α emission and minimizing the rich photochemistry of that species. Assuming that all neutral PAHs that disappear are converted into ions, an upper limit to the ionization efficiency can be obtained by measuring the percentage decrease in the integrated areas of the neutral bands upon photolysis. Ion yield upper limits ranging from 2 to 15% are typically realized with this technique. The upper limits of the yields for the spectra presented here were: fluoranthene, 8% and 11% (depending on electron acceptor; see below); benzo[*a*]fluoranthene, 8%; benzo[*b*]fluoranthene, 5%; benzo[*j*]fluoranthene, 11%; and benzo[*k*]fluoranthene, 6%. In those experiments involving benzo[*a*]fluoranthene and benzo[*j*]fluoranthene where both anions and cations are formed, it is assumed that the two are formed in roughly equal proportions, i.e., one anion forms for each cation produced.

All spectra reported here were measured at 0.5 cm^{-1} resolution by coadding 1000 individual scans using a Nicolet 740 Fourier transform infrared spectrometer. This level of resolution is critical for detecting ion bands which fall near the position of a neutral band, while the number of scans was chosen to optimize both the signal-to-noise ratio and time requirements of each experiment. Mid-infrared spectra (7000–500 cm^{-1}) were collected using a liquid nitrogen cooled MCT-B detector/KBr beam splitter combination. Individual experimental integrated band intensities ($\int \tau d\nu$) were determined using the OMNIC data analysis software package (Nicolet Instruments Corp.).

The PAHs used were obtained from several sources. Fluoranthene (98% purity) and benzo[*b*]fluoranthene (99% purity) were obtained from the Aldrich Chemical Co. Benzo[*k*]fluoranthene (99+% purity) was obtained from Janssen Chimica. Samples of benzo[*a*]fluoranthene and benzo[*j*]fluoranthene, were obtained from the Bureau of Community Reference (Brussels, Belgium; 98+% purity). All samples were used without further purification. Matheson ultrahigh purity argon (99.999% min.) was used for the matrix material.

B. Theoretical Methods. The geometries are optimized and the harmonic frequencies computed using density functional theory (DFT). Specifically, we use the hybrid¹³ B3LYP¹⁴ functional in conjunction with the 4-31G basis sets.¹⁵ Calibration calculations,^{4e} which have been carried out for selected systems, show that a single scale factor of 0.958 brings the B3LYP harmonic frequencies computed using the 4-31G basis set into reasonable agreement with the experimental fundamental frequencies. For example, in naphthalene the average absolute error is 4.4 cm^{-1} and the maximum error is 12.4 cm^{-1} . While the error can be reduced by increasing the basis set (provided the C–H stretches are scaled separately), the B3LYP/4-31G results are of sufficient accuracy to allow a critical evaluation of experiment. The calibration calculations also show that the computed B3LYP/4-31G intensities are accurate except for C–H stretches which are, on average, about a factor of 2 larger than those determined in the matrix studies.^{6d–f} While the gas-phase

data are very limited, it appears that the gas-phase intensities tend to lie between the matrix and B3LYP values. We also observe that when two or more bands of the same symmetry are close in energy, their relative intensities are sensitive to the level of theory, but that the *sum* of their intensities is relatively invariant and more reliable. In this regard, an analogous series of calculations using the BP86 functional were conducted. While the BP86 frequencies are expected to be less accurate than those of the B3LYP,¹⁶ the *distribution* of intensity between close lying modes provides insight into the stability of the B3LYP intensity distribution. All calculations were performed using the *Gaussian 94* computer code.¹⁷

III. Results

A detailed discussion of the means by which the experimentally measured PAH ion bands can be distinguished from those of other photoproducts has been presented previously.^{3b} Briefly, to be attributed to a PAH ion, a band must appear only when the associated neutral PAH is present in the matrix and only after photolysis. Its intensity must be directly and reproducibly proportional to the extent of PAH ionization and it must exhibit a constant ratio with respect to other bands attributed to the same species. To be associated with a PAH cation, the intensity of the band must be enhanced by the introduction of an electron acceptor to the matrix, while the bands of a PAH anion are, on the other hand, completely absent under such conditions. Finally, comparison with the theoretical calculated vibrational frequencies and intensities provides an important confirmation and furthermore permits assignment of an experimentally observed ion band. As was the case in previous studies,^{3b,6a-c} the intensities of the bands corresponding to the PAH cations peak after 4 to 8 min of photolysis and then remain essentially constant or fall off slightly upon further photolysis. Non-PAH related photoproduct bands are not common, numbering perhaps 2 to 4 in a typical experiment. The most common and prominent spurious photoproduct bands fall at 904 cm^{-1} (HAr_2^+)¹⁸ and 1589 cm^{-1} . The absence of any infrared bands attributable to PAH fragments as well as the presence of these two photoproduct bands in photolyzed Ar/ H_2O control experiments indicate that these bands are a product of contaminant water photolysis and are not due to PAH degradation. Less frequently, other weak photoproduct bands were encountered at 1388 and 1104 cm^{-1} (HO_2^+) and at 1039 cm^{-1} (O_3), as well as bands attributable to CO.

The mid-infrared spectra of the fluoranthene, benzo[*a*]fluoranthene, benzo[*b*]fluoranthene, benzo[*j*]fluoranthene, and benzo[*k*]fluoranthene cations are presented in the sections that follow. Only those regions of the spectrum where cation bands appear are shown. The experimentally measured band positions and relative intensities are tabulated and compared with the corresponding theoretical values in each subsection as well. The theoretical data presented in the tables have been truncated at the 1% relative intensity level. A complete listing of the calculated harmonic frequencies and intensities (both infrared active and inactive modes) can be found on the Internet at: <http://ccf.arc.nasa.gov/~cbauschl/astro.data5r>. In general, there is better agreement between the experimental and theoretical frequencies than is the case for their associated intensities. Consequently, the band assignments shown in the tables are primarily those correspondences which minimize frequency discrepancies. Deviations from this general practice are noted where appropriate.

A. Mid-Infrared Spectroscopy: Cations. 1. The Aromatic CH Stretching Region, 3200–2900 cm^{-1} . As has been the case with previous studies of PAH cations, no new features that could

be attributed to the aromatic CH stretching modes of any of the fluoranthene cations were observed upon photolysis. Experimental detection of new bands in this region is seriously complicated by heavy obscuration from the strong CH stretches and overtone and combination bands of the still-abundant, residual neutral PAH (see ref 6f). This difficulty is further exacerbated by the fact that the PAH cation bands in this region are predicted to be quite weak. Indeed, the theoretical calculations indicate that the modes in this region have absolute intensities only 10–30% that of the corresponding modes in the neutral species, and relative intensities of only a few percent when normalized to the strongest cation band. Thus, it is perhaps not surprising that these bands are not observed experimentally. Based on the signal-to-noise ratio of the experimental data and the reliability with which the pre-photolysis neutral spectrum can be subtracted from the post-photolysis spectrum, we estimate that the relative intensity of the aromatic CH stretching features of the cations reported here can be no more than 0.10. This is consistent with the theoretical results listed in the tables which predict that these modes have relative intensities in the 0.01 to 0.08 range.

2. The Fluoranthene Cation, $\text{C}_{16}\text{H}_{10}^+$. The mid-infrared spectrum of the fluoranthene cation is shown in Figure 2. Experimentally, the spectrum of this species proved to be particularly challenging to measure. First, experimental ion yields were very poor except in the presence of an electron acceptor. Second, the infrared bands of the fluoranthene cation are substantially weaker than those of the other PAH ions presented here. This is based on the qualitative observation that even in experiments with similar precursor neutral PAH concentrations and similar ionization efficiencies, the bands of the fluoranthene cation were much weaker and more difficult to discern than the bands of the other PAH cations considered in this study. Finally, an unusually high proportion of the bands of the fluoranthene cation fall at or near the position of neutral bands. To mitigate these difficulties here, the pre- and post-photolysis difference spectrum is shown in Figure 2. In addition, given the generally poor ion yields obtained by photolysis of neat Ar/fluoranthene samples, the spectra of fluoranthene cations generated with the assistance of an electron acceptor were used to prepare the figure. To get around the spectral obscurations of the electron acceptors discussed in section II.A above, the spectra from two such experiments, one employing CCl_4 , the other NO_2 , were combined to obtain one complete spectrum that is relatively free of obscuration. The portion of the spectrum from 1500 to 1100 cm^{-1} was measured in a CCl_4 -doped experiment (avoiding the strongest NO_2^- bands), while the spectrum from 1100 to 700 cm^{-1} was measured in an NO_2 -doped experiment (avoiding the strongest CCl_4 bands). The spectra were scaled to compensate for the modest differences in neutral abundance and ion yield between the two experiments.

The experimentally measured band frequencies and relative intensities are given in Table 1. In contrast to the rather good agreement between theory and experiment found for the benzofluoranthene ions described below, there is a marked disagreement between the two data sets for the fluoranthene cation. This discrepancy arises largely due to a symmetry-breaking artifact in the theoretical calculations caused by the mixing of the two lowest-lying electronic states of the cation which happen to fall very close in energy.¹⁶ This anomaly has been discussed in detail elsewhere and the theoretical data are not repeated here. The experimental data are included here for completeness and represent a distinct improvement over those earlier measurements.

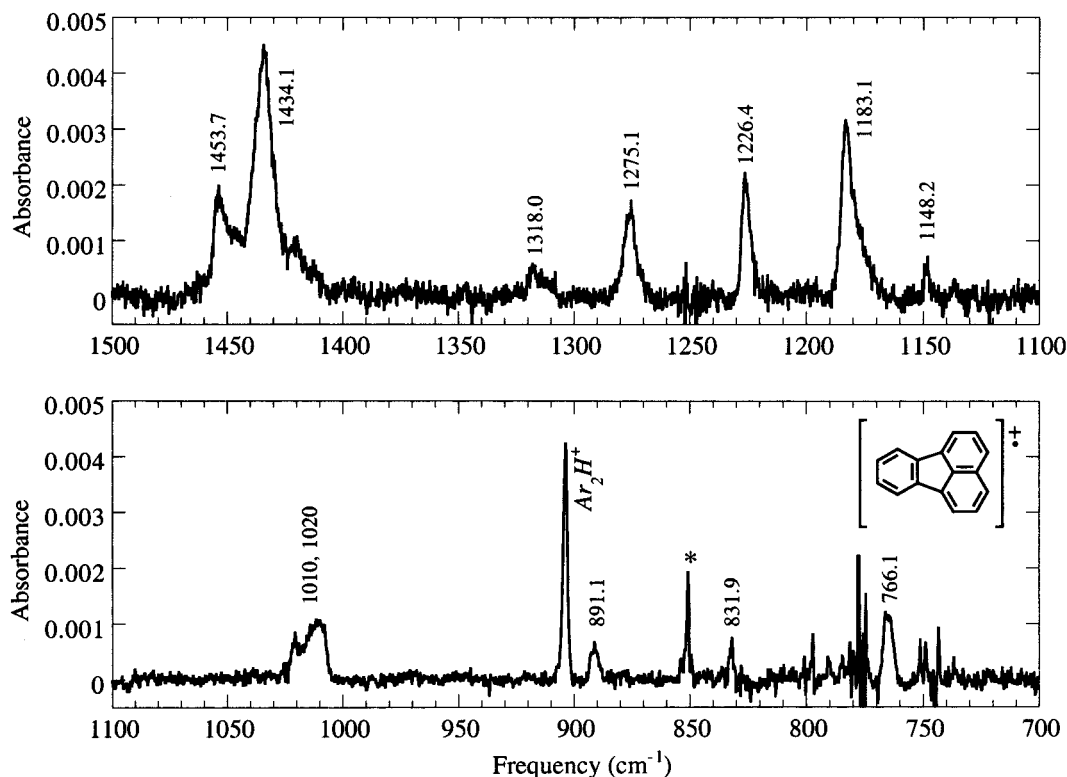


Figure 2. The experimentally measured mid-infrared spectrum of the fluoranthene cation ($C_{16}H_{10}^+$) isolated in an argon matrix at 12 K. This spectrum is the difference between the spectra of a fluoranthene/Ar sample measured before and after in situ Ly- α photolysis. The positions of the cation bands are labeled. The spectrum from 1500 to 1100 cm^{-1} was measured in the presence of the electron acceptor CCl_4 , while that from 1100 to 700 cm^{-1} was measured in the presence of NO_2 . Details of the marriage of these two spectra can be found in section III. A.2. The cation band at 676 cm^{-1} is not shown. The band marked with an asterisk (*) in the lower frame is an NO_2 photolysis product.

TABLE 1: Experimental Band Frequencies and Intensities for the Fluoranthene Cation

| frequency (cm^{-1}) | relative intensity |
|-------------------------|--------------------|
| 766.1 | 0.29 |
| 831.9 | 0.071 |
| 891.1 | 0.10 |
| 1010, 1020 | 0.45 |
| 1148.2 | 0.027 |
| 1183.1 | 0.68 |
| 1226.4 | 0.22 |
| 1275.1 | 0.18 |
| 1318.0 | 0.057 |
| 1434.1 | 1.0 |
| 1453.7 | 0.40 |

Inspection of the data in Figure 2 and Table 1 shows that the CC stretching and CH in-plane bending region between 1600 and 1100 cm^{-1} is dominated by strong bands at 1434.1 and 1183.1 cm^{-1} . Two new bands are observed in the CH out-of-plane bending region at 831.9 cm^{-1} and 766.1 cm^{-1} . Fluoranthene has two rings which contain three adjacent hydrogen atoms per ring and one with four adjacent H atoms (Figure 1). In the neutral molecule, the bands corresponding to these modes fall at 827.9 and 775.0 cm^{-1} (triply adjacent CH) and at 744.5 cm^{-1} (quadruply adjacent CH).^{6f} Based on the measured upper limit of 11% ionization achieved in the Ar/ NO_2 /fluoranthene experiment, and using the technique employed previously for other PAHs,^{6a-c} we estimate that the 831.7 cm^{-1} cation band is approximately three times weaker than the corresponding mode in the neutral molecule (827.9 cm^{-1}). Likewise, assuming the 766.1 cm^{-1} band corresponds to the quadruply adjacent CH out-of-plane mode, this band is suppressed by a factor of ~ 2 compared to the 744.5 cm^{-1} neutral band. If, instead, this cation band corresponds to the strong neutral 775.0 cm^{-1} band, its intensity is suppressed by $\sim 7\times$. Last, we attribute the 623.0

cm^{-1} band to a CCC out-of-plane bend due to its position below the low end of the frequency range normally associated with the CH out-of-plane bending modes in aromatic molecules.¹⁹

3. The Benzo[*a*]fluoranthene Cation. The mid-infrared spectrum of the matrix-isolated benzo[*a*]fluoranthene cation is presented in Figure 3. The experimentally measured difference spectrum is shown in black, with the positions of cation bands indicated in blue. The theoretically calculated spectrum is given by the blue trace above the experimental spectrum. The photoproduct bands marked in red and the red trace below the experimental data correspond to the benzo[*a*]fluoranthene anion and are discussed in section III. B.2 below.

The experimentally measured band frequencies and relative intensities are presented and compared with the theoretical values in Table 2. The experimental data have been normalized to the doublet cation band at 1352.3/1348.1 cm^{-1} rather than the strong complex of bands at 1407.5/1401.1/1395.2 cm^{-1} . This decision was made because the intensity of this complex is significantly larger than that of the theoretically predicted band at 1400.6 cm^{-1} . In all likelihood, this is an indication that the 1395.2 cm^{-1} band complex reflects the overlapping contributions of multiple cation vibrational modes rather than site-splitting of a single mode. Consequently, normalization to this complex results in a global underestimation of the relative intensities of the other cation bands. The choice to normalize to the 1352.3/1348.1 cm^{-1} was made because this is the second strongest feature in the experimental cation spectrum and because this band corresponds to the strongest predicted cation band at 1336.9 cm^{-1} .

The benzo[*a*]fluoranthene cation spectrum is very rich, with bands tending to fall in five groups. There is a cluster of moderately intense bands between 1600 and 1530 cm^{-1} arising

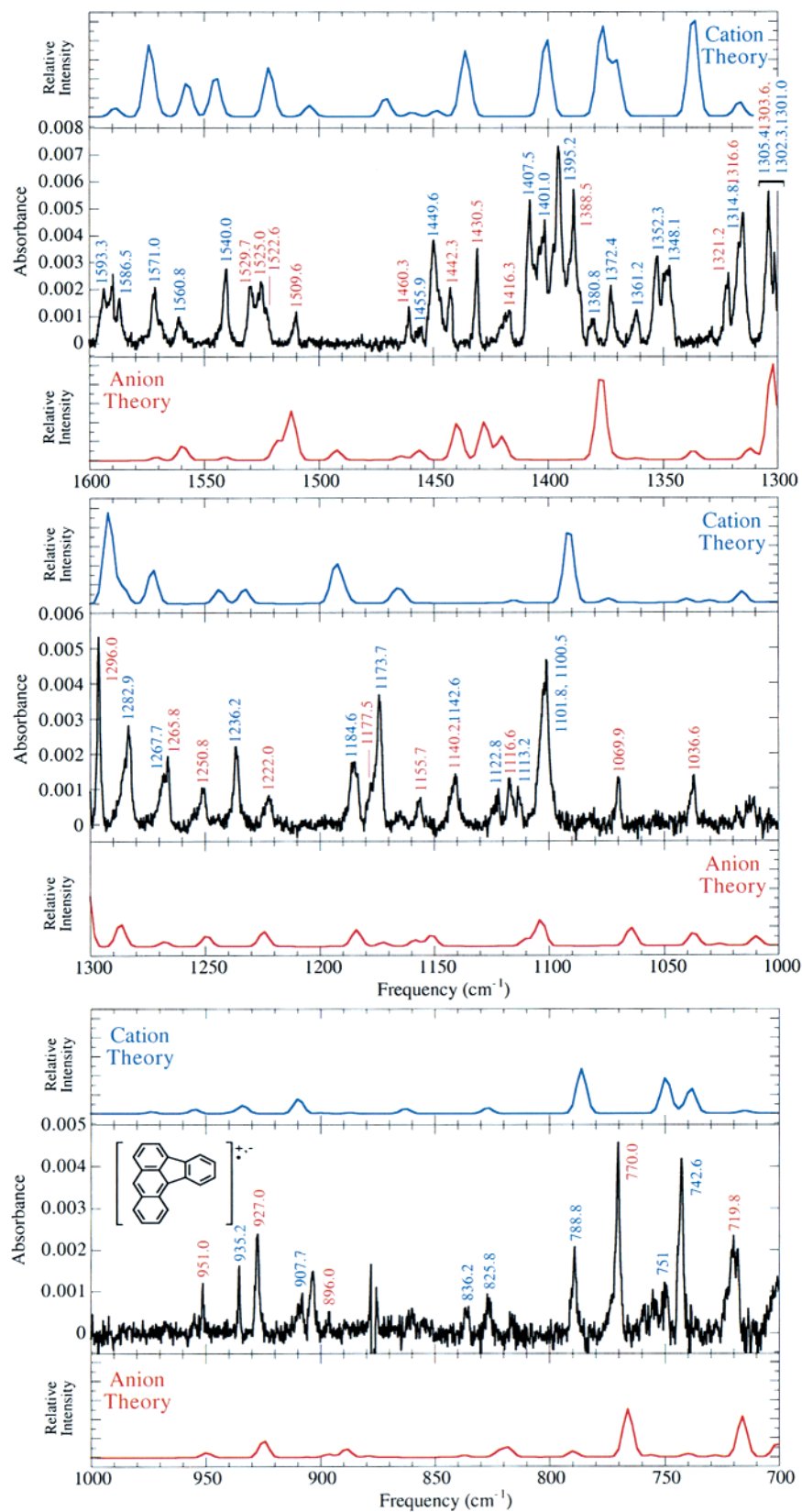


Figure 3. The theoretical and experimental mid-infrared spectra of the benzo[*a*]fluoranthene ($C_{20}H_{12}$) cation and anion. The experimental spectrum is the difference between the spectra of a benzo[*a*]fluoranthene/Ar sample measured before and after in situ Ly- α photolysis. The cation and anion data are color coded for clarity (cation, blue; anion, red), and the experimental bands are labeled with their positions. The cation band at 627.0 cm^{-1} is not shown.

from pure CC stretching vibrations; a cluster between 1425 and 1225 cm^{-1} which represents combinations of CC stretching and CH in-plane bending vibrations; a cluster between 1200 and 1100 cm^{-1} due to the CH in-plane bends; a group of two bands

near 900 cm^{-1} ; and a group between 850 and 750 cm^{-1} in the out-of-plane CH bending region. The theoretical calculations predict three bands at 1193.1 , 1190.8 , and 1189.5 cm^{-1} where two are observed experimentally (1184.6 and 1173.7 cm^{-1}). The

TABLE 2: Theoretical and Experimental Band Frequencies and Intensities for the Benzo[*a*]fluoranthene Cation

| sym | theory (B3LYP) | | | experiment | |
|-----|--------------------------|--------------------|--------------------|-----------------------------|--------------------|
| | freq (cm ⁻¹) | intensity (km/mol) | relative intensity | freq (cm ⁻¹) | relative intensity |
| A'' | 77.5 | 2.93 | 0.022 | | |
| A'' | 111.5 | 2.32 | 0.017 | | |
| A'' | 302.6 | 1.30 | 0.010 | | |
| A' | 339.8 | 2.35 | 0.017 | | |
| A'' | 463.5 | 7.07 | 0.053 | | |
| A' | 510.2 | 3.82 | 0.028 | | |
| A'' | 524.0 | 1.31 | 0.010 | | |
| A' | 578.0 | 2.11 | 0.016 | | |
| A'' | 583.3 | 6.79 | 0.050 | | |
| A' | 620.0 | 1.78 | 0.013 | | |
| A'' | 623.8 | 16.76 | 0.125 | 627.0 | 0.094 |
| A'' | 715.0 | 3.38 | 0.025 | | |
| A'' | 738.4 | 31.46 | 0.234 | 742.6 | 0.42 |
| A' | 742.0 | 3.83 | 0.028 | | |
| A'' | 749.5 | 46.08 | 0.342 | 751.2 | 0.21 |
| A'' | 786.0 | 57.45 | 0.427 | 788.8 | 0.19 |
| A' | 826.8 | 7.65 | 0.057 | 825.8 | 0.10 |
| A'' | 862.6 | 6.32 | 0.047 | 836.2 | 0.062 |
| A'' | 909.5 | 19.03 | 0.141 | 907.7 | 0.090 |
| A' | 933.5 | 10.19 | 0.076 | 935.2 | 0.085 |
| A'' | 938.2 | 2.18 | 0.016 | | |
| A' | 954.7 | 5.37 | 0.040 | | |
| A'' | 973.2 | 2.59 | 0.019 | | |
| A' | 1015.8 | 14.46 | 0.107 | | |
| A' | 1030.1 | 3.32 | 0.025 | | |
| A' | 1040.0 | 5.12 | 0.038 | | |
| A' | 1074.1 | 5.74 | 0.043 | | |
| A' | 1091.1 | 99.34 | 0.738 | 1100.5, 1101.8 | 0.84 |
| A' | 1115.0 | 3.72 | 0.028 | 1122.8, 1113.2 | 0.21 |
| A' | 1163.9 | 12.93 | 0.096 | 1142.6 | 0.074 |
| A' | 1167.0 | 12.69 | 0.094 | | |
| A' | 1189.5 | 17.92 | 0.133 | 1173.7 | 0.26 |
| A' | 1190.8 | 3.08 | 0.023 | | |
| A' | 1193.1 | 45.12 | 0.335 | 1184.6 | 0.26 |
| A' | 1232.5 | 18.99 | 0.141 | 1236.2 | 0.20 |
| A' | 1243.6 | 18.20 | 0.135 | | |
| A' | 1272.5 | 44.45 | 0.330 | 1267.7 | 0.13 |
| A' | 1285.4 | 22.06 | 0.164 | 1282.9 | 0.43 |
| A' | 1291.7 | 118.30 | 0.879 | 1301.0, 1302.3, 1305.4 | 0.36 |
| A' | 1316.7 | 18.63 | 0.138 | 1314.8 | 0.40 |
| A' | 1336.9 | 134.55 | 1.000 | 1348.1, 1352.3 ^a | 1.0 |
| A' | 1370.5 | 73.41 | 0.546 | 1361.2 | 0.17 |
| A' | 1376.6 | 118.00 | 0.877 | 1372.4 | 0.24 |
| | | | | 1380.8 | 0.12 |
| A' | 1400.6 | 102.55 | 0.762 | 1395.2, 1401.1, 1407.5 | 2.4 |
| A' | 1435.2 | 43.52 | 0.323 | | |
| A' | 1436.5 | 45.36 | 0.337 | | |
| A' | 1448.5 | 7.56 | 0.056 | 1449.6 | 0.59 |
| A' | 1459.2 | 5.29 | 0.039 | 1455.9 | 0.059 |
| A' | 1470.8 | 24.23 | 0.180 | | |
| A' | 1504.1 | 14.10 | 0.105 | | |
| A' | 1521.7 | 63.73 | 0.474 | | |
| A' | 1544.9 | 53.08 | 0.395 | 1540.0 | 0.31 |
| A' | 1557.3 | 44.94 | 0.334 | 1560.8 | 0.13 |
| A' | 1570.0 | 5.02 | 0.037 | 1571.0 | 0.25 |
| A' | 1573.7 | 92.72 | 0.689 | 1586.5 | 0.091 |
| A' | 1588.6 | 11.49 | 0.085 | 1593.3 | 0.28 |
| A' | 3075.7 | 1.31 | 0.010 | | |
| A' | 3097.0 | 10.48 | 0.078 | | |
| A' | 3099.1 | 8.52 | 0.063 | | |
| A' | 3102.0 | 3.26 | 0.024 | | |
| A' | 3108.4 | 8.89 | 0.066 | | |
| A' | 3132.7 | 7.26 | 0.054 | | |

^aNormalized to experimental 1348.1/1352.3 band in agreement with theory.

assignments given in the table were selected to given the best agreement in band intensity. Note that while the discrepancies in the relative intensities of the individual bands in this cluster

are as large as a factor of 2, the total theoretically predicted and experimentally measured intensities are in good agreement (theory: 0.491; experiment: 0.52).

There are six bands observed in the 925 to 675 cm⁻¹ region, four of which are assigned to a'' CH out-of-plane bending vibrations. Since this molecule has two rings with quadruply adjacent H atoms, one with triply adjacent hydrogens, and one with a nonadjacent hydrogen atom, several bands would be expected. These are slightly shifted out of the normal regions expected for specific hydrogen atoms in a manner consistent with that found for PAHs containing only fused hexagonal rings.²⁰ Except for the 836.2 cm⁻¹ band which differs by an unusually large 30 cm⁻¹ from predictions, there is generally good agreement between theoretical and experimental frequencies across this region, with the rest falling within 4 cm⁻¹ of each other. While there is substantial scatter in the relative intensities of the individual CH out-of-plane bending features between theory and experiment, the total intensities of all bands assigned to this class of mode are in reasonably good agreement (theory: 1.19; experiment, 0.97). Based on the results of several experiments both with and without electron acceptors, we estimate that the intensity of the nonadjacent CH out-of-plane bending mode of the benzo[*a*]fluoranthene cation (907.7 cm⁻¹) is suppressed by a factor of ~3 from the corresponding mode in the neutral molecule (876.7 cm⁻¹).^{6f} Likewise, the intensity of the 742.6 cm⁻¹ quadruply adjacent mode is suppressed by a factor of ~2 in the cation compared to the 739.0 cm⁻¹ neutral band.^{6f} The remaining two CH out-of-plane bending features at 788.8 and 751.2 cm⁻¹ are not significantly affected by ionization compared to their neutral counterparts (783.0 and 750.2 cm⁻¹).^{6f}

Regarding the rest of the spectrum, comparison of the frequencies listed in Table 2 shows that there is generally good agreement between theory and experiment in this case, with most theoretical peak frequencies falling within 2 to 10 cm⁻¹ of the experimental values and all falling within 21 cm⁻¹. While somewhat greater discrepancies in relative intensity are observed between the experimental and theoretical bands, the overall agreement between the two data sets is still reasonably good. As was the case in the CH out-of-plane bending region discussed above, discrepancies can often be traced back to differences in the distribution of intensity between two or more close-lying modes, with the sum of the intensities of the associated modes showing much better agreement.

4. The Benzo[*b*]fluoranthene Cation. The mid-infrared spectrum of the benzo[*b*]fluoranthene cation is shown in Figure 4 with the experimentally measured band frequencies and relative intensities compared with the theoretical values in Table 3.

The experimentally measured benzo[*b*]fluoranthene cation spectrum is not nearly so rich as is the case for the other benzofluoranthene cations. Given the low symmetry of the molecule (C_s), it is unlikely that this is merely due to a significantly lower occurrence of infrared active vibrational modes in this cation. Certainly this is not the case for the neutral molecule.^{6f} Instead, it is more likely that an unhappy confluence of experimental effects combine to make the ion bands particularly difficult to detect. First, the ionization efficiencies obtained in experiments with this species were significantly lower (e.g., 5% for the spectrum in Figure 4) than those achieved for the other molecules in this study. In addition, a qualitative comparison between the spectrum of the benzo[*b*]fluoranthene cation and those of the other benzofluoranthene cations indicates that the bands of this cation are intrinsically weaker than those of the other cations. Finally, as was the case with the fluoran-

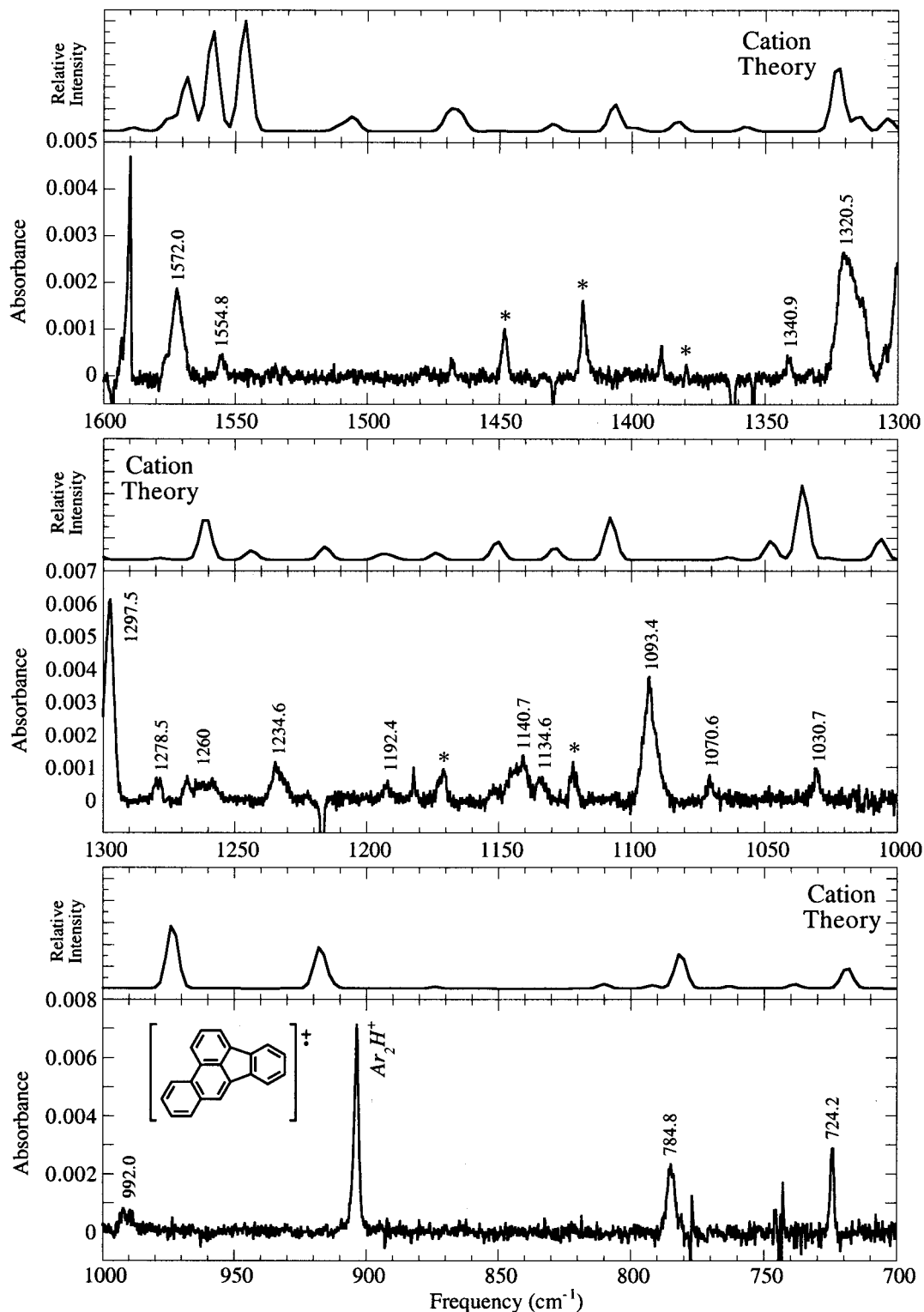


Figure 4. The theoretical and experimental mid-infrared spectra of the benzo[*b*]fluoranthene cation ($C_{20}H_{12}^+$). The experimental spectrum is the difference between the spectra of a benzo[*b*]fluoranthene/Ar sample measured before and after in situ Ly- α photolysis. The cation bands are labeled with their positions. The cation bands at 583.3 and 589.6 cm^{-1} are not shown. The bands marked with asterisks (1447.3, 1417.9, 1379.0, 1170.6, 1121.6 cm^{-1}) are possible anion features.

these cation discussed above, it may also be that an unusually high proportion of the cation bands are obscured under the bands of the remaining neutral benzo[*b*]fluoranthene.

As before, the bands can be grouped according to the type of fundamental vibrational mode involved. There is a moderately intense CC stretching band at 1572.0 cm^{-1} ; a group between 1345 and 1230 cm^{-1} corresponding to combinations of CC stretching and CH in-plane bending vibrations; a group distrib-

uted over the range from 1200 to 990 cm^{-1} due at least in part to CH in-plane bending; two bands at 784.8 and 724.2 cm^{-1} in the CH out-of-plane bending region; and a pair at 589.6 and 583.3 cm^{-1} corresponding to skeletal deformation modes. Of particular note, theory predicts four moderate to strong bands at 1546.3, 1558.5, 1568.3, and 1575.0 cm^{-1} , where only two experimental bands are observed (1554.8 and 1572.0 cm^{-1}). The assignments shown in Table 3 give the best frequency agree-

TABLE 3: Theoretical and Experimental Band Frequencies and Intensities for the Benzo[*b*]fluoranthene Cation

| sym | theory (B3LYP) | | | experiment | |
|-----|--------------------------|--------------------|--------------------|--------------------------|--------------------|
| | freq (cm ⁻¹) | intensity (km/mol) | relative intensity | freq (cm ⁻¹) | relative intensity |
| A' | 153.3 | 5.27 | 0.018 | | |
| A' | 257.7 | 7.89 | 0.027 | | |
| A' | 312.8 | 21.31 | 0.073 | | |
| A' | 384.0 | 10.71 | 0.037 | | |
| A'' | 439.0 | 3.57 | 0.012 | | |
| A' | 460.2 | 38.24 | 0.131 | | |
| A' | 538.2 | 19.43 | 0.067 | | |
| A' | 552.7 | 28.92 | 0.099 | | |
| A' | 590.2 | 10.88 | 0.037 | 583.3 | 0.071 |
| A' | 603.6 | 38.02 | 0.131 | 589.6 | 0.11 |
| A' | 647.5 | 6.46 | 0.022 | | |
| A'' | 718.8 | 55.84 | 0.192 | 724.2 | 0.18 |
| A'' | 738.5 | 10.63 | 0.037 | | |
| A'' | 762.9 | 5.64 | 0.019 | | |
| A'' | 781.3 | 89.95 | 0.309 | 784.8 | 0.20 |
| A' | 782.0 | 3.67 | 0.013 | | |
| A' | 791.9 | 9.12 | 0.031 | | |
| A'' | 810.1 | 12.00 | 0.041 | | |
| A'' | 874.1 | 4.49 | 0.015 | | |
| A'' | 913.7 | 12.84 | 0.044 | | |
| A' | 917.6 | 107.89 | 0.371 | | |
| A' | 973.4 | 167.56 | 0.576 | 992.0 | 0.042 |
| A' | 1006.3 | 54.97 | 0.189 | | |
| A' | 1026.4 | 6.12 | 0.021 | | |
| A' | 1035.7 | 195.75 | 0.673 | 1030.7 | 0.063 |
| A' | 1047.7 | 49.93 | 0.172 | | |
| A' | 1063.4 | 6.78 | 0.023 | 1070.6 | 0.036 |
| A' | 1107.8 | 111.07 | 0.382 | 1093.4 | 0.60 |
| A' | 1128.8 | 32.45 | 0.112 | 1134.6 | 0.075 |
| A' | 1150.6 | 48.87 | 0.168 | 1140.7 | 0.12 |
| A' | 1173.7 | 18.00 | 0.062 | | |
| A' | 1191.1 | 11.39 | 0.039 | 1192.4 | 0.054 |
| A' | 1195.0 | 12.16 | 0.042 | | |
| A' | 1215.8 | 34.68 | 0.119 | | |
| A' | 1243.7 | 24.45 | 0.084 | 1234.6 | 0.12 |
| A' | 1261.0 | 114.72 | 0.394 | 1260 ^a | 0.29 |
| A' | 1278.4 | 4.42 | 0.015 | 1278.5 | 0.054 |
| A' | 1303.8 | 35.14 | 0.121 | 1297.5 | 1.0 |
| A' | 1314.8 | 40.58 | 0.139 | | |
| A' | 1322.9 | 178.82 | 0.614 | 1320.5 | 0.51 |
| A' | 1357.2 | 12.53 | 0.043 | 1340.9 | 0.032 |
| A' | 1382.7 | 26.61 | 0.091 | | |
| A' | 1398.8 | 9.52 | 0.033 | | |
| A' | 1406.5 | 71.96 | 0.247 | | |
| A' | 1429.7 | 19.71 | 0.068 | | |
| A' | 1464.9 | 45.14 | 0.155 | | |
| A' | 1469.0 | 50.14 | 0.172 | | |
| A' | 1505.5 | 37.65 | 0.129 | | |
| A' | 1510.5 | 15.06 | 0.052 | | |
| A' | 1546.3 | 291.03 | 1.000 | | |
| A' | 1558.5 | 266.69 | 0.916 | 1554.8 | 0.033 |
| A' | 1568.3 | 141.57 | 0.486 | 1572.0 | 0.21 |
| A' | 1575.0 | 34.64 | 0.119 | | |
| A' | 1588.7 | 8.22 | 0.028 | | |
| A' | 3074.9 | 4.30 | 0.015 | | |
| A' | 3089.6 | 4.41 | 0.015 | | |
| A' | 3100.4 | 11.76 | 0.040 | | |
| A' | 3102.9 | 20.70 | 0.071 | | |
| A' | 3106.0 | 10.38 | 0.036 | | |

^a Broad band with complex profile.

ment, but there is clearly a serious discrepancy between the total theoretical and experimental relative intensities (theory: 2.521; experiment: 0.24) that is uncharacteristic among strong bands.

Since this molecule has two rings with quadruply adjacent H atoms, one with triply adjacent hydrogens, and one with a nonadjacent hydrogen atom, several bands would be expected

in the CH out-of-plane bending region. Thus, some cation bands in this region must be weak and/or obscured. Inspection of the theoretical data in Table 3 does show that the other undetected *a''* modes in this region are weaker than the two detected bands. The two bands that are observed fall in the regions associated with trio (784.8 cm⁻¹) and quartet (724.2 cm⁻¹) modes. These two bands agree within 6 cm⁻¹ of the theoretically predicted vibrations; however, there is again substantial scatter in the relative intensities. Based on the measured upper limit of 5% ionization, we estimate that the intensity of the 784.8 cm⁻¹ triply adjacent CH out-of-plane bending mode is suppressed by a factor of ~2 from the corresponding mode in the neutral molecule (777.4 cm⁻¹).^{6f} The 724.2 cm⁻¹ quadruply adjacent mode is not significantly affected by ionization compared to the 735.7 cm⁻¹ mode of neutral benzo[*b*]fluoranthene.^{6f}

Regarding the rest of the spectrum, comparison of the theoretical and experimental frequencies listed in Table 2 shows that, as in the previous case, most theoretical peak frequencies are between 2 and 10 cm⁻¹ of the experimental values, with three falling within 21 cm⁻¹. Again, however, relative intensities do vary significantly.

Finally, it is interesting to note the presence of a weak family of photoproduct bands that appear in Figure 4 at 1447.3, 1417.9, 1379.0, 1170.6, and 1121.6 cm⁻¹ (noted with an asterisk). These bands are associated with benzo[*b*]fluoranthene and may be attributable to the anion. However, if this is the case, they are substantially weaker relative to the cation than is the case for the benzo[*a*]- and benzo[*j*]fluoranthene anions discussed below. Given the experimental difficulties encountered with this molecule and the diminutive intensities of the bands in question, a definitive assignment of this family of bands will require further study.

5. The Benzo[*j*]fluoranthene Cation. The mid-infrared spectrum of the matrix-isolated benzo[*j*]fluoranthene cation is presented in Figure 5. The experimentally measured difference spectrum is shown in black, with the positions of cation bands indicated in blue. The theoretically calculated spectrum is given by the blue trace above the experimental spectrum. The photoproduct bands marked in red and the red trace below the experimental data correspond to the benzo[*j*]fluoranthene anion, and are discussed in section III. B.3 below. The experimentally measured band frequencies and relative intensities are compared with the theoretical values in Table 4.

While the theoretical spectrum of the benzo[*j*]fluoranthene cation is simpler than that of the benzo[*b*]fluoranthene cation, the experimental spectrum is far richer, presumably due to less cation band overlap with neutral benzo[*j*]fluoranthene bands. Again the bands can be sorted into five groups corresponding to the fundamental vibrations of aromatic hydrocarbons. Those falling at 1575.6 and 1550.8 cm⁻¹ can be assigned to the pure CC stretching vibrations, while those lying between 1504.7 and perhaps 1200 cm⁻¹ can be attributed to combinations of CC stretching and CH in-plane bending vibrations. The bands at 1153.1 and 1120.2 cm⁻¹ can be attributed to CH in-plane bends. The small cluster between 1060.2 and 1090.1 cm⁻¹ are likely due to a combination of CC and CH character, and those at 826.4, 792.9, 769.0, and 743.8 cm⁻¹ to the out-of-plane CH bends. The assignments of the experimental bands at 1575.6, 1397.9, and 1210.1 cm⁻¹ shown in Table 4 give substantially better agreement between the experimental and theoretical relative intensities than if the assignments are made purely on the basis of frequency. Also, the BP86 solution spreads the intensity between the theoretical 1333.1 and 1326.1 cm⁻¹ bands, strengthening the assignments shown in the table.

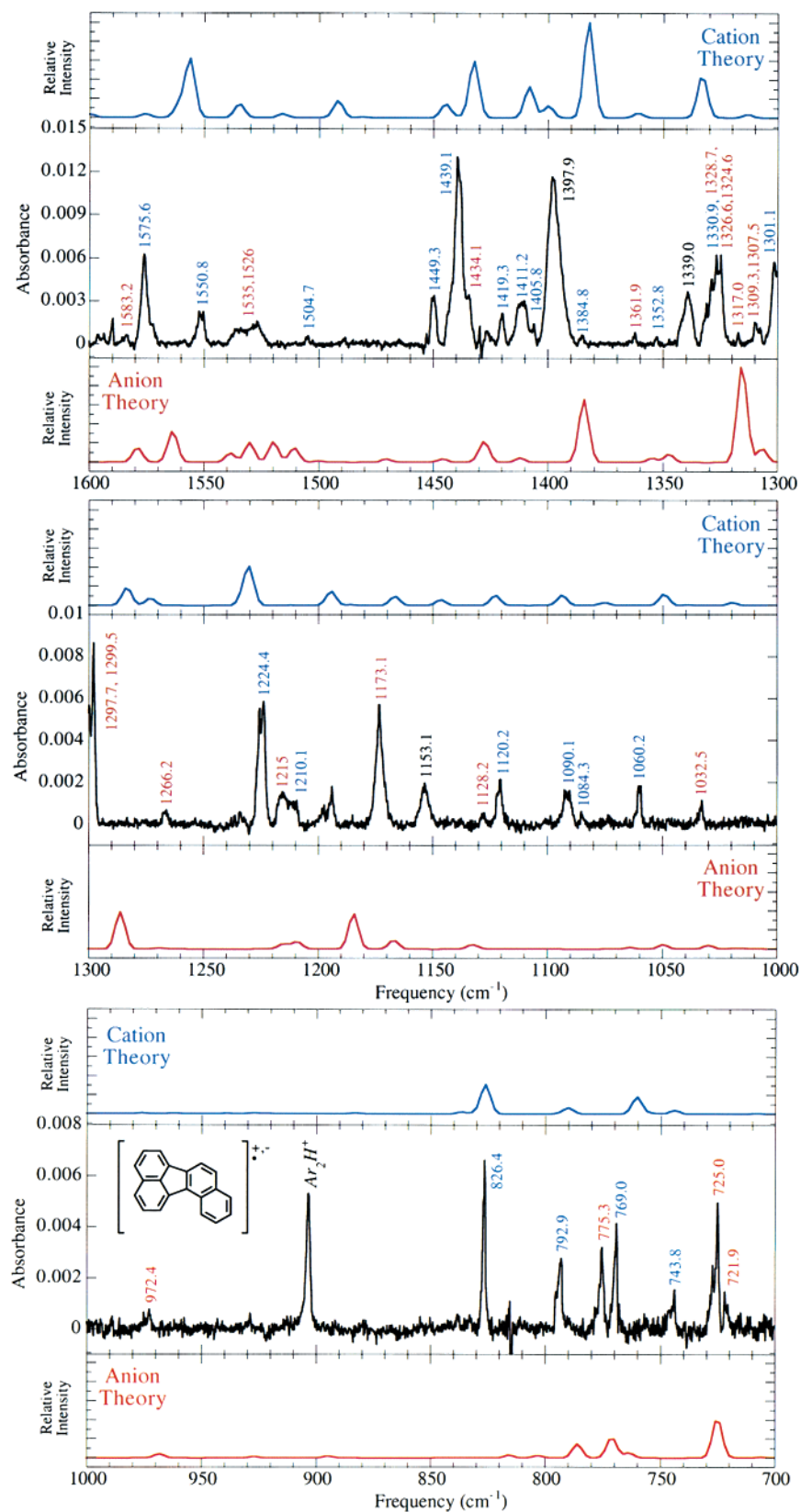


Figure 5. Comparison of the theoretical and experimental mid-infrared spectra of the benzo[*j*]fluoranthene (C₂₀H₁₂) cation and anion. The experimental spectrum is the difference between the spectra of a benzo[*j*]fluoranthene/Ar sample measured before and after in situ Ly- α photolysis. The cation and anion bands are labeled with their positions and color coded for clarity (cation, blue; anion, red). The black labels at 1397.9, 1339.0, and 1153.1 cm⁻¹ indicate bands with unresolved contributions from both the cation and the anion.

There are four bands detected in the 925–675 cm⁻¹ region, but only three, those at 826.4, 769.0, and 743.8 cm⁻¹, have the proper symmetry (a'') to be CH out-of-plane vibrations. Since this molecule has one ring with quadruply adjacent CH groups,

two with equivalent triply adjacent CH groups, and one with a doubly adjacent CH group, this is the minimum number of bands that might be expected. The band at 826.4 cm⁻¹ falls squarely in the region associated with the CH out-of-plane vibration of

TABLE 4: Theoretical and Experimental Band Frequencies and Intensities for the Benzo[j]fluoranthene Cation

| sym | theory (B3LYP) | | | experiment | |
|-----|--------------------------|--------------------|--------------------|--------------------------|--------------------|
| | freq (cm ⁻¹) | intensity (km/mol) | relative intensity | freq (cm ⁻¹) | relative intensity |
| A'' | 168.2 | 5.23 | 0.016 | | |
| A' | 334.5 | 4.27 | 0.013 | | |
| A' | 480.7 | 5.77 | 0.018 | | |
| A'' | 489.1 | 10.81 | 0.033 | | |
| A' | 507.0 | 3.75 | 0.012 | | |
| A'' | 519.6 | 4.67 | 0.014 | | |
| A' | 543.7 | 7.26 | 0.022 | | |
| A' | 570.0 | 9.46 | 0.029 | | |
| A'' | 744.0 | 12.10 | 0.037 | 743.8 | 0.052 |
| A'' | 760.3 | 56.36 | 0.173 | 769.0 | 0.11 |
| A' | 790.1 | 20.82 | 0.064 | 792.9 | 0.091 |
| A'' | 826.1 | 99.51 | 0.305 | 826.4 | 0.14 |
| A'' | 836.6 | 6.92 | 0.021 | | |
| A' | 1019.7 | 9.29 | 0.029 | | |
| A' | 1049.4 | 37.70 | 0.116 | 1060.2 | 0.10 |
| A' | 1075.3 | 9.63 | 0.030 | 1084.3 | 0.015 |
| A' | 1093.6 | 34.55 | 0.106 | 1090.1 | 0.070 |
| A' | 1122.6 | 35.09 | 0.108 | 1120.2 | 0.077 |
| A' | 1146.5 | 19.69 | 0.060 | 1153.1 | 0.11 |
| A' | 1166.5 | 31.13 | 0.096 | | |
| A' | 1194.5 | 48.75 | 0.150 | 1210.1 | 0.030 |
| A' | 1211.4 | 1.84 | 0.006 | | |
| A' | 1230.1 | 122.19 | 0.375 | 1224.4 | 0.29 |
| A' | 1232.9 | 26.09 | 0.080 | | |
| A' | 1273.1 | 24.32 | 0.075 | | |
| A' | 1283.3 | 60.42 | 0.185 | 1301.1 | 0.39 |
| A' | 1313.0 | 11.64 | 0.036 | | |
| A' | 1326.1 | 1.63 | 0.005 | 1330.9 | 0.088 |
| A' | 1333.1 | 145.81 | 0.447 | 1339.0 | 0.23 |
| A' | 1361.0 | 16.12 | 0.049 | 1352.8 | 0.013 |
| | | | | 1384.8 | 0.021 |
| A' | 1382.3 | 325.84 | 1.000 | 1397.9 | 1.0 |
| A' | 1399.8 | 40.91 | 0.126 | 1405.8 | 0.013 |
| A' | 1408.1 | 105.14 | 0.323 | 1411.2 | 0.16 |
| | | | | 1419.3 | 0.073 |
| A' | 1432.3 | 193.08 | 0.593 | 1439.1 | 0.74 |
| A' | 1438.6 | 3.85 | 0.012 | | |
| A' | 1444.6 | 46.94 | 0.144 | 1449.3 | 0.12 |
| A' | 1491.7 | 57.71 | 0.177 | 1504.7 | 0.013 |
| A' | 1516.0 | 12.58 | 0.039 | | |
| A' | 1534.7 | 46.94 | 0.144 | | |
| A' | 1556.2 | 197.88 | 0.607 | 1550.8 | 0.12 |
| A' | 1561.0 | 45.08 | 0.138 | 1575.6 | 0.33 |
| A' | 1575.7 | 11.85 | 0.036 | | |
| A' | 1599.9 | 10.30 | 0.032 | | |
| A' | 3090.0 | 5.49 | 0.017 | | |
| A' | 3097.0 | 11.19 | 0.034 | | |
| A' | 3101.1 | 5.57 | 0.017 | | |
| A' | 3107.3 | 4.91 | 0.015 | | |
| A' | 3130.9 | 5.73 | 0.018 | | |

doubly adjacent hydrogen atoms. Likewise, the 769.0 cm⁻¹ absorption can be assigned to the triply adjacent CH vibration, and the 743.8 cm⁻¹ band to the quadruply adjacent mode. The positional agreement between theory and experiment is very good for these modes, all falling within 10 cm⁻¹ of their predicted positions. In this case, the measured relative intensities are in good agreement with predictions. Based on the measured upper limit of 11% ionization, we estimate that the intensity of the CH out-of-plane bending modes of the benzo[j]fluoranthene cation bands at 826.4, 769.0, and 743.8 cm⁻¹ are all suppressed by a factor of ~2 from their corresponding modes in the neutral molecule (815.5, 769.2, and 738.7 cm⁻¹, respectively).^{6f}

Regarding the rest of the spectrum, comparison of the theoretical and experimental frequencies and relative intensities listed in Table 4 shows that there is generally good agreement between theory and experiment with most differences falling

between 2 and 10 cm⁻¹ of the experimental values, and all fall within 20 cm⁻¹. The magnitude of the variations between the experimentally measured and theoretically predicted relative band intensities is similar to that observed for the other cations considered here.

6. *The Benzo[k]fluoranthene Cation.* The mid-infrared spectrum of the benzo[k]fluoranthene cation is shown in Figure 6, together with a synthetic representation of the theoretically calculated spectrum. The experimentally measured band frequencies and relative intensities are presented and compared with the theoretical values in Table 5. Interestingly, despite the higher symmetry of this molecule (C_{2v}), the benzo[k]fluoranthene cation exhibits the richest spectrum of all of the ions considered in this work. While this is partly due to less cation band overlap with neutral benzo[k]fluoranthene bands, more important is the striking intensity of the infrared bands of this cation, particularly in the CC stretching and CH in-plane bending regions. Despite having an ionization efficiency lower than all but the benzo[b]fluoranthene experiments (6%), the bands of this cation are among the most intense observed in any of our studies of matrix-isolated PAH cations to date. The spectrum is so rich that it is difficult to separate the bands clearly into the specific regions normally associated with aromatic hydrocarbon fundamental mode vibrations and no attempt is made to do so. It should be noted that the assignments of the 1582.6/1578.4, 1571.8, and 1292.3 cm⁻¹ bands given in Table 5 give significantly better agreement between the theoretical and experimental relative intensities than is the case if the assignments are made on the basis of frequency alone. Also, the band at 674.6 cm⁻¹ could equally well be assigned to either of the theoretical bands at 683.4 and 663.0 cm⁻¹.

The experimental data shown in Table 5 were initially normalized to the remarkably intense 1320.7 cm⁻¹ cation band which does correspond to the strongest theoretically predicted band (1321.5 cm⁻¹). However, when the resulting relative intensities were compared to the theoretical values, they were found to be uniformly smaller by a factor of 2–3. Renormalizing the data to make the sum of the relative intensities of the experimental bands at 1582.6, 1578.4, 1571.8, and 1561.9 cm⁻¹ equal to that of the 1587.2, 1565.5, and 1559.1 cm⁻¹ theoretical bands largely neutralized this discrepancy. These bands were chosen because they are moderately intense and because they arise in a relatively clean portion of the experimental spectrum. It was decided to normalize to the summed intensity of several close-lying bands rather than that of a single band in an effort to improve the accuracy of the result. As discussed above, while there are often marked discrepancies between theory and experiment in the distribution of intensity among the individual bands of a cluster, the total intensities are often in much better agreement. The implication here is that the experimental 1320.7 cm⁻¹ bands is almost three times more intense than the theoretical 1321.5 cm⁻¹ band. Such a discrepancy is unusual for a strong PAH cation band. The profile of this band (see Figure 6) does suggest the presence of more than one component. However, inspection of the data in Table 5 shows that there are no nearby, unaccounted-for theoretical bands of appreciable intensity, so this substructure may simply be due to site-splitting of a single, very intense mode.

There are six bands detected in the range from 925 to 675 cm⁻¹, three of which have the symmetry of CH out-of-plane bending modes (a₂ or b₁). Since this molecule has one ring with quadruply adjacent H atoms, two equivalent rings with triply adjacent hydrogens, and one with two, equivalent, nonadjacent hydrogen atoms, several bands would be expected. Although

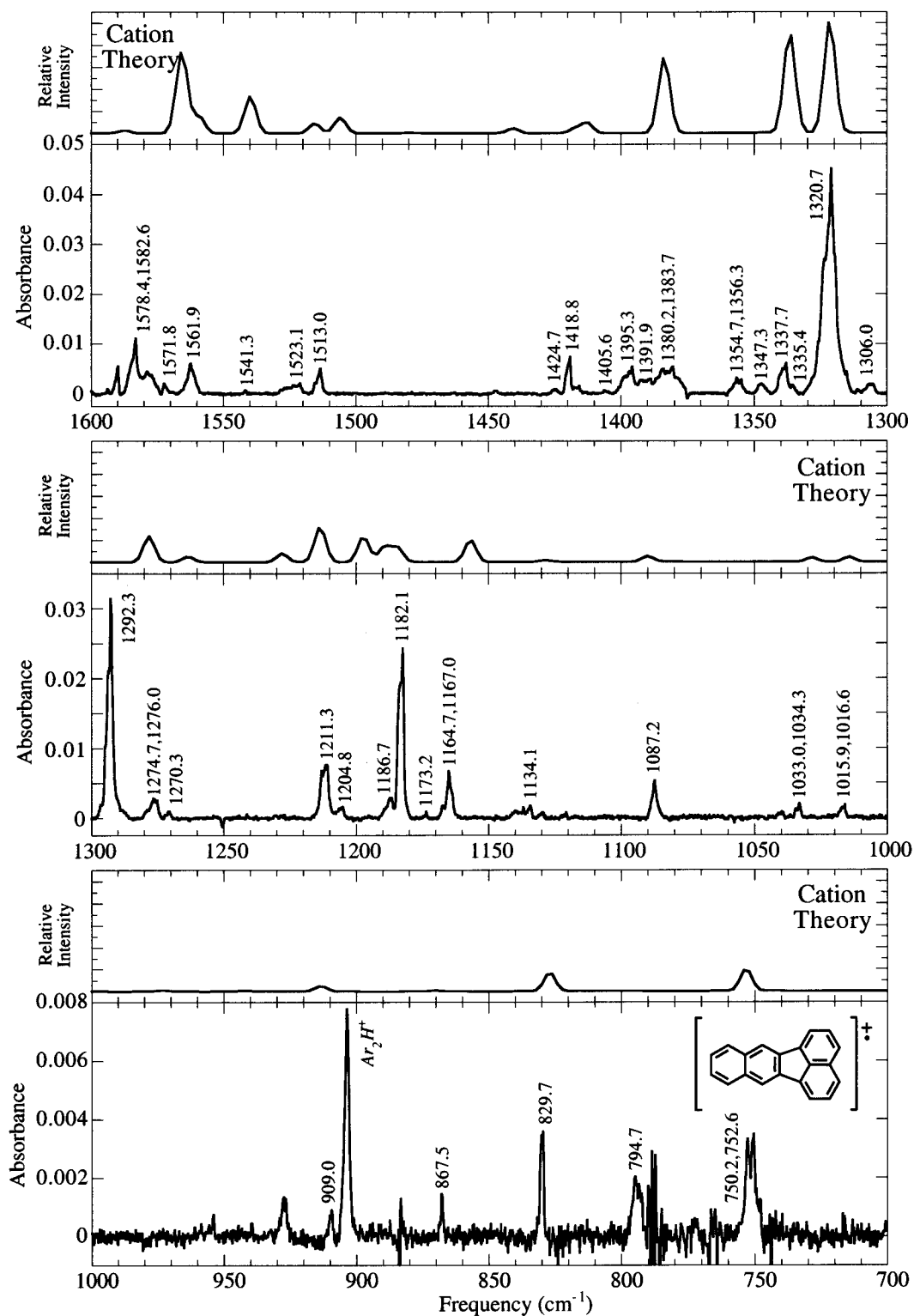


Figure 6. The theoretical and experimental mid-infrared spectra of the benzo[k]fluoranthene (C₂₀H₁₂) cation. The experimental spectrum is the difference between the spectra of a benzo[k]fluoranthene/Ar sample measured before and after in situ Ly- α photolysis. The cation bands are labeled with their positions. The band at 674.6 cm⁻¹ is not shown.

specific assignments require closer analysis of the theoretical results, it seems reasonable to attribute the 752.3/750.2 cm⁻¹ absorption to a quartet vibration, the 794.7 and 829.7 cm⁻¹ bands to a splitting of the two equivalent trio vibrations, and the 909.0 cm⁻¹ feature to the solo mode. There is good agreement between theory and experimental frequencies for all of these bands, with the largest difference being 5 cm⁻¹. There is also moderately good agreement between relative intensities. Based on the measured upper limit of 6% ionization, we estimate

that the intensity of the CH out-of-plane bending modes at 909.0 and 829.7 cm⁻¹ are suppressed by factors of ~ 3 and ~ 2 relative to the corresponding modes in the neutral molecules (883.5 and 823.7 cm⁻¹, respectively).^{6f} The cation modes at 794.7 and 752.3/750.2 cm⁻¹ bands are not significantly affected by ionization.

Regarding the rest of the spectrum, comparison of the theoretical and experimental frequencies and relative intensities listed in Table 5 shows that there is remarkably good agreement

TABLE 5: Theoretical and Experimental Band Frequencies and Intensities for the Benzo[*k*]fluoranthene Cation

| sym | theory (B3LYP) | | | experiment | |
|-----|--------------------------|--------------------|--------------------|--------------------------|--------------------|
| | freq (cm ⁻¹) | intensity (km/mol) | relative intensity | freq (cm ⁻¹) | relative intensity |
| B1 | 447.4 | 14.33 | 0.034 | | |
| A1 | 553.2 | 5.46 | 0.013 | | |
| A1 | 600.6 | 6.80 | 0.016 | | |
| A1 | 663.0 | 4.93 | 0.012 | | |
| B2 | 683.4 | 4.28 | 0.010 | 674.6 | 0.014 |
| B1 | 753.1 | 82.42 | 0.193 | 750.2, 752.6 | 0.15 |
| A1 | 803.3 | 1.39 | 0.003 | 794.7 | 0.037 |
| B1 | 826.9 | 71.05 | 0.166 | 829.7 | 0.079 |
| B2 | 869.7 | 4.29 | 0.010 | 867.5 | 0.018 |
| B1 | 913.0 | 19.19 | 0.045 | 909.0 | 0.027 |
| B1 | 972.8 | 4.98 | 0.012 | | |
| B2 | 1014.3 | 17.66 | 0.041 | 1015.9, 1016.6 | 0.035 |
| A1 | 1028.3 | 16.49 | 0.039 | 1033.0, 1034.3 | 0.038 |
| B2 | 1089.8 | 21.77 | 0.051 | 1087.2 | 0.16 |
| B2 | 1128.3 | 5.84 | 0.014 | 1134.1 | 0.060 |
| B2 | 1156.7 | 83.21 | 0.195 | 1164.7, 1167.0 | 0.18 |
| A1 | 1184.3 | 56.05 | 0.131 | 1173.2 | 0.013 |
| B2 | 1189.2 | 59.75 | 0.140 | 1182.1 | 0.67 |
| A1 | 1197.1 | 97.29 | 0.228 | 1186.7 | 0.060 |
| | | | | 1204.8 | 0.036 |
| A1 | 1213.4 | 133.94 | 0.314 | 1211.3 | 0.28 |
| B2 | 1227.8 | 33.08 | 0.077 | | |
| B2 | 1263.3 | 21.35 | 0.050 | 1270.3 | 0.023 |
| | | | | 1274.7, 1276.0 | 0.13 |
| A1 | 1278.0 | 97.47 | 0.228 | 1292.3 | 1.0 |
| | | | | 1306.0 | 0.075 |
| A1 | 1321.5 | 427.07 | 1.000 | 1320.7 | 2.9 |
| B2 | 1336.0 | 15.23 | 0.036 | 1335.4 | 0.014 |
| A1 | 1336.7 | 368.77 | 0.864 | 1337.7 | 0.25 |
| B2 | 1347.5 | 0.93 | 0.002 | 1347.3 | 0.083 |
| | | | | 1354.7, 1356.3 | 0.14 |
| A1 | 1383.6 | 288.32 | 0.675 | 1380.2, 1383.7 | 0.33 |
| | | | | 1391.9 | 0.011 |
| | | | | 1395.3 | 0.18 |
| A1 | 1412.6 | 40.31 | 0.094 | 1405.6 | 0.014 |
| B2 | 1417.2 | 17.06 | 0.040 | 1418.8 | 0.21 |
| A1 | 1440.5 | 19.44 | 0.046 | 1424.7 | 0.030 |
| A1 | 1505.9 | 60.88 | 0.143 | 1513.0 | 0.14 |
| B2 | 1515.5 | 37.48 | 0.088 | 1523.1 | 0.12 |
| A1 | 1539.7 | 139.76 | 0.327 | 1541.3 | 0.009 |
| B2 | 1559.1 | 65.45 | 0.153 | 1561.9 | 0.25 |
| A1 | 1565.5 | 311.97 | 0.730 | 1578.4, 1582.6 | 0.62 |
| A1 | 1587.2 | 11.89 | 0.028 | 1571.8 | 0.038 |
| B2 | 3096.2 | 10.90 | 0.026 | | |
| A1 | 3096.5 | 15.39 | 0.036 | | |
| A1 | 3102.4 | 17.92 | 0.042 | | |

between theory and experiment with most differences falling between 0 and 10 cm⁻¹. The difference is greater only for the 1424.7 cm⁻¹, which is only 15 cm⁻¹ from the theoretical value. As in all other cases reported here, the relative intensity differences are more variable.

B. Mid-Infrared Spectroscopy: Anions. During the course of our studies of matrix-isolated benzo[*a*]fluoranthene and benzo[*j*]fluoranthene, it became clear that there was a second, distinct class of PAH-related photoproduct bands appearing in the spectrum. This second class of bands satisfied all of the aforementioned criteria to be classified as a PAH ion except that, instead of being enhanced by the presence of an electron acceptor in the matrix, they were completely suppressed. Based on this behavior, and the overall similarity in the pattern of frequencies and intensities displayed by these bands to those of the PAH cation, we attribute these features to the anions of the parent PAH. Subsequent theoretical calculations of the vibrational spectra of the benzo[*a*] and benzo[*j*]fluoranthene anions confirm this assignment. The concurrent formation of PAH cation/anion pairs under photolysis in matrix-isolation

experiments is not unprecedented, having been reported previously for the PAH pentacene.^{6b,7a} It is interesting that under similar experimental conditions two of the benzofluoranthenes produce anions, while for the other two little or no anions are produced. Presumably this stems from differences in the electron affinities of the various species, although it is not clear why there would be marked discrepancies in this quantity between the various isomers. This behavior would suggest that there is an electron affinity threshold that must be overcome for the production of PAH anion/cation pairs by long-range electron transfer in a matrix to occur. However, assigning a numerical value to that hypothetical threshold would require more extensive study and reliable values for the electron affinities of the PAHs.

1. The Aromatic CH Stretching Region, 3200–2900 cm⁻¹.

Unlike the situation with the cations in which theory predicts very weak aromatic CH stretching bands between 3150 and 3000 cm⁻¹, inspection of Tables 6 and 7 shows that the corresponding anion bands are expected to be some of the strongest in the spectrum. Indeed, the total intensity of these modes is predicted to be about a factor of 3 more intense than the corresponding modes in the neutral molecules. This interesting theoretical result is borne out by our detection of the corresponding absorption in the experimental spectra. These observations are illustrated in Figure 7 which shows the difference between the pre- and post-photolysis spectra of benzo[*a*] and benzo[*j*]fluoranthene samples in the absence of an electron acceptor. It should be emphasized here that despite heavy interference from neutral absorptions in this region, these features are not merely artifacts of the subtraction process. The position, profile, and relative intensity of these features have been reproduced in multiple experiments in the absence of an electron acceptor. No similar features are observed in the presence of an electron acceptor, nor are they observed in the spectra of fluoranthene, benzo[*b*] and benzo[*k*]fluoranthene where no anions are produced. The broad, 50 cm⁻¹ fwhh band in the spectrum of the benzo[*a*]fluoranthene anion peaks near the predicted position of the strongest theoretical bands in this region (3038.4 and 3036.9 cm⁻¹) and its envelope encompasses all of the calculated bands which span the range from 3004.8 to 3094.4 cm⁻¹. The same is true for the benzo[*j*]fluoranthene anion, whose broad absorption envelope spans the range from about 3010 cm⁻¹ to 3090 cm⁻¹, encompassing most of the theoretically predicted features between 3001.0 and 3084.3 cm⁻¹. Given the uncertainty associated with the theoretically calculated intensities in this region (section II.B), as well as that associated with the experimental band areas measured from such heavily obscured bands, it is impossible to make a quantitative comparison of the theoretically predicted and experimentally measured relative intensities. The two data sets do, however, appear to be in at least in qualitative agreement in this respect.

2. The Benzo[*a*]fluoranthene Anion. The experimentally measured mid-infrared spectrum of the benzo[*a*]fluoranthene anion can be found in Figure 3, together with its cation spectrum discussed in section III. A.3 above. The positions of the anion bands are indicated in red, with a synthetic representation of the theoretically calculated spectrum shown by the red trace below the experimental data. The measured band frequencies and relative intensities are presented and compared with their theoretically calculated values in Table 6. As with the cations, inspection of Table 6 shows that there is significantly better agreement between the theoretical and experimental band frequencies than the relative intensities. Most measured positions differ from predicted positions by less than 5 cm⁻¹. Such

TABLE 6: Theoretical and Experimental Band Frequencies and Intensities for the Benzo[a]fluoranthene Anion

| sym | theory (B3LYP) | | | experiment | |
|-----|--------------------------|--------------------|--------------------|--------------------------|--------------------|
| | freq (cm ⁻¹) | intensity (km/mol) | relative intensity | freq (cm ⁻¹) | relative intensity |
| A' | 268.4 | 3.44 | 0.025 | | |
| A'' | 423.8 | 1.56 | 0.012 | | |
| A'' | 470.8 | 3.76 | 0.028 | | |
| A' | 515.7 | 2.96 | 0.022 | | |
| A'' | 593.4 | 2.43 | 0.018 | | |
| A'' | 608.1 | 4.54 | 0.034 | | |
| A' | 627.2 | 2.26 | 0.017 | | |
| A' | 678.0 | 1.52 | 0.011 | | |
| A'' | 700.8 | 19.11 | 0.141 | | |
| A'' | 716.2 | 56.49 | 0.418 | 719.8 | 0.34 |
| A'' | 728.0 | 2.26 | 0.017 | | |
| A' | 739.9 | 4.85 | 0.036 | | |
| A'' | 755.9 | 3.23 | 0.024 | | |
| A'' | 766.0 | 67.07 | 0.496 | 770.0 | 0.35 |
| A'' | 789.7 | 8.09 | 0.060 | | |
| A' | 817.9 | 12.48 | 0.092 | | |
| A'' | 822.0 | 7.74 | 0.057 | | |
| A'' | 837.0 | 2.62 | 0.019 | | |
| A'' | 878.6 | 2.25 | 0.017 | | |
| A' | 888.7 | 12.18 | 0.090 | | |
| A'' | 896.6 | 4.65 | 0.034 | 896.0 | 0.031 |
| A' | 924.7 | 23.66 | 0.175 | 927.0 | 0.18 |
| A' | 949.6 | 6.52 | 0.048 | 951.0 | 0.044 |
| A' | 1010.0 | 13.07 | 0.097 | | |
| A' | 1026.1 | 2.95 | 0.022 | | |
| A' | 1037.3 | 18.62 | 0.138 | 1036.6 | 0.12 |
| A' | 1064.4 | 25.87 | 0.191 | 1069.6 | 0.084 |
| A' | 1103.6 | 36.63 | 0.271 | 1116.6 | 0.14 |
| A' | 1109.8 | 10.18 | 0.075 | | |
| A' | 1151.1 | 15.79 | 0.117 | 1140.2 | 0.075 |
| A' | 1158.2 | 9.00 | 0.067 | 1155.7 | 0.073 |
| A' | 1172.3 | 5.65 | 0.042 | | |
| A' | 1184.0 | 22.97 | 0.170 | 1177.5 | 0.27 |
| A' | 1224.4 | 21.14 | 0.156 | 1222.0 | 0.092 |
| A' | 1249.2 | 15.06 | 0.111 | 1250.8 | 0.090 |
| A' | 1267.5 | 6.99 | 0.052 | 1265.8 | 0.14 |
| A' | 1286.7 | 32.36 | 0.239 | 1296.0 | 0.34 |
| A' | 1302.4 | 135.17 | 1.000 | 1303.6 | 0.40 |
| A' | 1312.1 | 15.87 | 0.117 | 1316.6 | 0.31 |
| A' | 1336.9 | 12.86 | 0.095 | 1321.2 | 0.14 |
| A' | 1361.7 | 2.54 | 0.019 | | |
| A' | 1370.4 | 3.81 | 0.028 | | |
| A' | 1377.0 | 123.98 | 0.917 | 1388.5 | 1.0 |
| A' | 1420.0 | 32.96 | 0.244 | 1416.3 | 0.16 |
| A' | 1427.7 | 53.17 | 0.393 | 1430.5 | 0.19 |
| A' | 1439.5 | 52.09 | 0.385 | 1442.3 | 0.11 |
| A' | 1456.1 | 13.63 | 0.101 | 1460.3 | 0.072 |
| A' | 1464.1 | 5.63 | 0.042 | | |
| A' | 1492.2 | 13.84 | 0.102 | 1509.6 | 0.10 |
| A' | 1512.0 | 68.03 | 0.503 | 1522.6, 1525.0, 1529.7 | 0.55 |
| A' | 1518.2 | 26.54 | 0.196 | | |
| A' | 1540.8 | 4.83 | 0.036 | | |
| A' | 1559.3 | 20.84 | 0.154 | | |
| A' | 1570.9 | 4.85 | 0.036 | | |
| A' | 3001.0 | 16.28 | 0.120 | | |
| A' | 3004.4 | 3.69 | 0.027 | | |
| A' | 3012.6 | 10.59 | 0.078 | | |
| A' | 3017.1 | 32.79 | 0.243 | | |
| A' | 3020.4 | 47.43 | 0.351 | | |
| A' | 3021.7 | | 0.599 | | |
| A' | 3036.9 | 143.81 | 1.06 | | |
| A' | 3038.4 | 285.30 | 2.11 | 3036, 3058 | 2.3 |
| A' | 3041.0 | 12.05 | 0.089 | | |
| A' | 3057.5 | 29.64 | 0.219 | | |
| A' | 3084.3 | 45.22 | 0.335 | | |

agreement holds for the benzo[j]fluoranthene anion as well, suggesting that the B3LYP method is as applicable for the calculation of harmonic frequencies and intensities of PAH

TABLE 7: Theoretical and Experimental Band Frequencies and Intensities for the Benzo[j]fluoranthene Anion

| sym | theory (B3LYP) | | | experiment | |
|-----|--------------------------|--------------------|--------------------|--------------------------|--------------------|
| | freq (cm ⁻¹) | intensity (km/mol) | relative intensity | freq (cm ⁻¹) | relative intensity |
| A'' | 427.8 | 2.82 | 0.014 | | |
| A' | 481.7 | 13.51 | 0.065 | | |
| A' | 521.1 | 5.57 | 0.027 | | |
| A' | 571.7 | 4.16 | 0.020 | | |
| A' | 640.8 | 2.99 | 0.014 | | |
| A'' | 667.9 | 3.98 | 0.019 | | |
| A'' | 717.5 | 0.81 | 0.004 | 721.9 | 0.093 |
| A'' | 725.1 | 84.56 | 0.408 | 725.0 | 0.37 |
| A'' | 763.6 | 10.89 | 0.053 | | |
| A'' | 771.0 | 44.10 | 0.213 | 775.3 | 0.26 |
| A'' | 785.8 | 17.54 | 0.085 | | |
| A' | 786.0 | 12.08 | 0.058 | | |
| A'' | 803.1 | 5.01 | 0.024 | | |
| A'' | 815.5 | 6.26 | 0.030 | | |
| A'' | 894.9 | 4.18 | 0.020 | | |
| A' | 926.9 | 3.46 | 0.017 | | |
| A' | 968.2 | 8.51 | 0.041 | 972.4 | 0.017 |
| A' | 1017.0 | 2.04 | 0.010 | | |
| A' | 1029.9 | 7.82 | 0.038 | 1032.5 | 0.083 |
| A' | 1049.7 | 9.72 | 0.047 | | |
| A' | 1064.1 | 3.54 | 0.017 | | |
| A' | 1129.7 | 2.81 | 0.014 | 1128.2 | 0.043 |
| A' | 1133.1 | 8.54 | 0.041 | | |
| A' | 1166.8 | 18.92 | 0.091 | 1153.1 | 0.089 |
| A' | 1184.4 | 74.66 | 0.360 | 1173.1 | 0.59 |
| A' | 1208.9 | 15.20 | 0.073 | | |
| A' | 1213.5 | 5.49 | 0.026 | | |
| A' | 1215.8 | 7.02 | 0.034 | 1215 | 0.23 |
| A' | 1269.0 | 2.71 | 0.013 | 1266.2 | 0.046 |
| A' | 1286.0 | 78.32 | 0.378 | 1297.7, 1299.5 | 0.29 |
| A' | 1306.7 | 29.62 | 0.143 | 1307.5, 1309.3 | 0.12 |
| | | | | 1317.0 | 0.021 |
| A' | 1315.4 | 207.27 | 1.000 | 1324.6, 1326.6, 1328.7 | 1.0 |
| A' | 1347.4 | 17.14 | 0.083 | 1339.0 | 0.24 |
| A' | 1354.8 | 9.06 | 0.044 | 1361.9 | 0.28 |
| A' | 1384.2 | 132.78 | 0.641 | 1397.9 | 0.51 |
| A' | 1411.9 | 9.13 | 0.044 | | |
| A' | 1427.4 | 41.38 | 0.200 | 1434.1 | 0.14 |
| A' | 1429.7 | 4.88 | 0.024 | | |
| A' | 1445.7 | 7.05 | 0.034 | | |
| A' | 1470.3 | 7.01 | 0.034 | | |
| A' | 1499.9 | 3.19 | 0.015 | | |
| A' | 1510.6 | 30.54 | 0.147 | | |
| A' | 1519.6 | 42.90 | 0.207 | 1526, 1535 | 0.50 |
| A' | 1530.0 | 41.21 | 0.199 | | |
| A' | 1538.4 | 19.05 | 0.092 | | |
| A' | 1563.5 | 65.41 | 0.316 | | |
| A' | 1578.8 | 30.65 | 0.148 | 1583.2 | 0.057 |
| A' | 2998.3 | 37.30 | 0.180 | | |
| A' | 2999.5 | 14.89 | 0.072 | | |
| A' | 3004.8 | 5.45 | 0.026 | | |
| A' | 3007.4 | 4.19 | 0.020 | | |
| A' | 3019.2 | 39.78 | 0.192 | | |
| A' | 3020.7 | 16.14 | 0.078 | | |
| A' | 3027.6 | 116.52 | 0.562 | | |
| A' | 3031.5 | 106.33 | 0.513 | | |
| A' | 3036.7 | 195.75 | 0.944 | 3035 | 3.9 |
| A' | 3043.5 | 124.16 | 0.599 | | |
| A' | 3059.2 | 26.41 | 0.127 | | |
| A' | 3094.4 | 31.13 | 0.150 | | |

anions as has been the case for the cations. Apart from the very strong band strength enhancement for the CH stretch in the anion, the overall pattern of intensities over the rest of the spectrum resembles that observed in the cations, indicating a similar dramatic enhancement in the CC stretching and CH in-plane bending modes in the anion. Of particular note, theory predicts three bands at 1518.2, 1512.0, and 1492.2 cm⁻¹. In

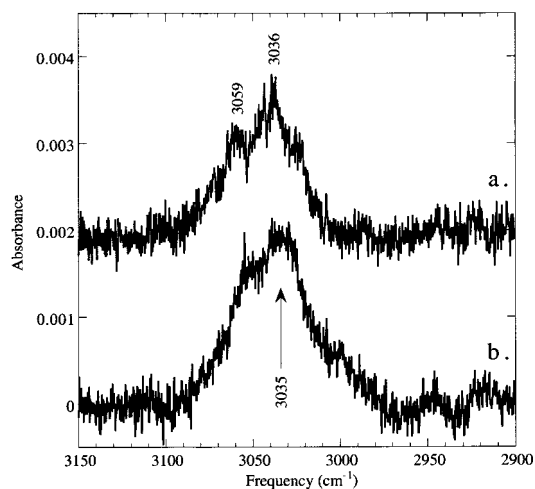


Figure 7. The spectra of the benzo[*a*]fluoranthene and benzo[*j*]fluoranthene anions through the aromatic CH stretching region. The spectra were generated by taking the difference between the pre- and post-photolysis spectra used to prepare Figures 3 and 5. The positions of the major absorption components are indicated.

this same region, experiment shows a triplet with maxima at 1529.7/1525.0/1522.6 cm^{-1} and a lone band at 1509.6 cm^{-1} . The assignment shown in Table 6 gives the best overall intensity agreement; the exact band-to-band correspondences remain in question. Nevertheless, once again, the total theoretically predicted and experimentally measured relative intensities through these bands are in reasonably good agreement (theory: 0.801; experiment: 0.65).

Of particular interest are the band positions in the CH out-of-plane region between 925 and 675 cm^{-1} . Three anion bands are observed in this region. The band at 896.0 cm^{-1} is assigned to the nonadjacent CH out-of-plane mode, the one at 770.0 is assigned to the triply adjacent mode, and the one at 719.8 cm^{-1} is assigned to the quadruply adjacent mode. The 19 cm^{-1} blue shift in the nonadjacent mode from the corresponding neutral position (876.7 cm^{-1})^{6f} is similar to, if somewhat smaller than, that observed in the cation (30 cm^{-1}). The 20 cm^{-1} blue shift in the 770.0 cm^{-1} band (neutral: 750.2 cm^{-1})^{6f} and the 31 cm^{-1} red shift in the 719.8 cm^{-1} band (neutral 740.8 cm^{-1})^{6f} are much larger than those observed in the corresponding cations, and uncharacteristically large for triply and quadruply adjacent CH out-of-plane bending modes in PAH cations in general.²⁰ Based on the upper limit of 8% ionization, and assuming a 1:1 ratio in the production of anions and cations, it appears that the 896.0 and 719.8 cm^{-1} anion bands are suppressed by factors of ~ 5 and ~ 2 , respectively, compared to the corresponding modes in the neutral molecules. The 770.0 cm^{-1} band, on the other hand, is enhanced by a factor of ~ 2 compared to the corresponding neutral mode.

3. The Benzo[*j*]fluoranthene Anion. The experimentally measured mid-infrared spectrum of the benzo[*j*]fluoranthene anion can be found in Figure 5, together with its cation spectrum discussed in section III. A.5 above. The positions of the anion bands are indicated in red, with a synthetic representation of the theoretically calculated spectrum shown by the red trace below the experimental data. The measured band frequencies and relative intensities are presented and compared with their theoretically calculated values in Table 7. For the benzo[*j*]fluoranthene anion, as with all of the other ions considered here, there is significantly better agreement between the theoretical and experimental band frequencies than the relative intensities. Most measured positions differ from predicted positions by less than 10 cm^{-1} . Apart from the enhancement of the CH stretching

modes in the anion discussed above, the characteristics of the rest of the spectrum are very similar to those of the cations. Both the CC stretching and CH in-plane bending modes between about 1600 and 1200 cm^{-1} undergo significant enhancement with respect to the neutral species and have comparable values in both ionization forms. The CH out-of-plane bending modes also have comparable strengths in both ionization states.

In the 925–675 cm^{-1} aromatic CH out-of-plane bending region, three bands attributable to the benzo[*j*]fluoranthene anion have been observed. These fall at 775.3, 725.0, and 721.9 cm^{-1} , and all are assigned to bands with the a'' symmetry of out-of-plane bends. The band at 775.3 cm^{-1} corresponds to the out-of-plane bending of the two triply adjacent CH groups, while those at 725.0 and 721.9 cm^{-1} fall in the range that is usually characteristic of quadruply adjacent CH groups. No band is observed experimentally that might be attributed to the expected doubly adjacent mode, but inspection of the theoretical calculations shows that this feature is expected to be weak. Following an analysis analogous to that employed for the other PAH ions, we estimate the 775.3 cm^{-1} band is suppressed by a factor of ~ 3 relative to its neutral counterpart at 769.2 cm^{-1} .^{6f} On the other hand, the 725.0/721.9 cm^{-1} pair (assuming they arise from a splitting of a single mode) is not significantly affected by ionization compared to the corresponding neutral mode (738.7 cm^{-1}).^{6f} While the direction of the shifts in these modes is the same as that observed for the benzo[*a*]fluoranthene anion (triply adjacent, blue shift; quadruply adjacent, red shift), the magnitudes of the shifts are substantially less (5 and 14 cm^{-1} , respectively).

V. Conclusions

The experimental and theoretical mid-infrared spectra of the fluoranthene ($\text{C}_{16}\text{H}_{10}$), benzo[*a*]fluoranthene, benzo[*b*]fluoranthene, benzo[*j*]fluoranthene, and benzo[*k*]fluoranthene (all $\text{C}_{20}\text{H}_{12}$ isomers) cations are presented. In addition, the spectra of the anions of benzo[*a*]fluoranthene and benzo[*j*]fluoranthene are also reported. The experimental data have all been obtained using the matrix-isolation technique, and the theoretical values have all been determined using the B3LYP approach. As has been the case with previous PAH cation experimental studies and consistent with theoretical predictions, no new features were measured in the CH stretch region between 3200 and 2900 cm^{-1} , due to severe overlap with the stronger parent bands.

The strongest mid-infrared absorption bands of these PAH cations fall between 1600 and about 1100 cm^{-1} corresponding to the CC stretching and CH in-plane modes. The most intense of these tend to fall between 1500 and 1300 cm^{-1} . These modes are 2–10 times stronger than the bands due to the CH out-of-plane bending modes in the 925 to 675 cm^{-1} range. This relationship is opposite that observed for neutral PAHs (in which the CH out-of-plane modes are the more intense by a factor of 2–10) and is similar to the trend observed in the ions of PAHs composed only of fused hexagonal ring.

With the exception of fluoranthene, there is good overall agreement between theory and experiment. The failure of the B3LYP approach for fluoranthene¹⁶ appears to arise from the symmetry breaking which occurs due the mixing of the two lowest-lying electronic states.

Acknowledgment. The authors acknowledge the expert technical support of Bob Walker, and valuable scientific discussions with Max Bernstein, Farid Salama, and Scott Sandford. This work was fully supported by NASA's Laboratory Astrophysics and Long Term Space Astrophysics programs, under grants #188-44-57-01 and #399-20-01-05.

References and Notes

- (1) (a) Allamandola, L. J.; Tielens, A. G. G. M.; Barker, J. R. *Ap. J. Supp. Ser.* **1989**, *71*, 733. (b) Puget, J. L.; Leger, A. *Annu. Rev. Astron. Astrophys.* **1989**, *27*, 161. (c) Allamandola, L. J. In *Topics in Current Chemistry*; Cyvin, S., Gutman, J., Eds.; Springer-Verlag, Berlin, 1990; p 1. (d) Allamandola, L. J.; Hudgins, D. M.; Sandford, S. A. *Ap. J. Lett.*, **1999**, *511*, L115.
- (2) Allamandola, L. J.; Tielens, A. G. G. M.; Barker, J. R. *Ap. J. Lett.* **1985**, *290*, L25.
- (3) (a) Szczepanski, J.; Roser, D.; Personette, W.; Eyring, M.; Pellow, R.; Vala, M. *J. Phys. Chem.* **1992**, *96*, 7876. (b) Hudgins, D. M.; Sandford, S. A.; Allamandola, L. J. *J. Phys. Chem.* **1994**, *98*, 4243. (c) d'Hendecourt, L. B.; Leger, A. In *The First Symposium on the Infrared Cirrus and Diffuse Interstellar Clouds, ASP Conference Series Vol. 58*; Cutri, R. M., Latter, W. B., Eds.; Astronomical Society of the Pacific: San Francisco, 1994. (d) Cook, D. J.; Saykally, R. J. *Ap. J. Lett.* **1998**, *493*, 793. (e) Piest, H.; von Helden, G.; Meijer, G. *Ap. J. Lett.* **1999**, *520*, L75.
- (4) (a) DeFrees, D. J.; Miller, M. D. In *Interstellar Dust: Contributed Papers*; Allamandola, L. J., Tielens, A. G. G. M., Eds.; NASA CP 3036, 1989; p 173. (b) Pauzat, F.; Talbi, D.; Miller, M. D.; DeFrees, D. J.; Ellinger, Y. *J. Phys. Chem.* **1992**, *96*, 7882. (c) DeFrees, D. J.; Miller, M. D.; Talbi, D.; Pauzat, F.; Ellinger, Y. *Ap. J. Lett.* **1993**, *408*, 530. (d) Langhoff, S. R. *J. Phys. Chem.* **1996**, *100*, 2819. (e) Bauschlicher, C. W., Jr.; Langhoff, S. R. *Spectrochim. Acta A* **1997**, *53*, 1225. (f) Langhoff, S. R.; Bauschlicher, C. W., Jr.; Hudgins, D. M.; Sandford, S. A.; Allamandola, L. J. *J. Phys. Chem. A* **1998**, *102*, 1632.
- (5) (a) Szczepanski, J.; Vala, M.; Talbi, D.; Parisel, O.; Ellinger, Y. *J. Chem. Phys.* **1993**, *98*, 4494. (b) Szczepanski, J.; Chapo, C.; Vala, M. *Chem. Phys. Lett.* **1993**, *205*, 434. (c) Szczepanski, J.; Vala, M. *Astrophys. J.* **1993**, *414*, 179. (d) Vala, M.; Szczepanski, J.; Pauzat, F.; Parisel, O.; Talbi, D.; Ellinger, Y. *J. Phys. Chem.* **1994**, *98*, 9187. (e) Szczepanski, J.; Drawdy, J.; Wehlburg, C.; Vala, M. *Chem. Phys. Lett.* **1995**, *245*, 539.
- (6) (a) Hudgins, D. M.; Allamandola, L. J. *J. Phys. Chem.* **1995**, *99*, 3033. (b) Hudgins, D. M.; Allamandola, L. J. *J. Phys. Chem.* **1995**, *99*, 8978. (c) Hudgins, D. M.; L. J. Allamandola, *J. Phys. Chem. A* **1997**, *101*, 3472. (d) Hudgins D. M.; Sandford, S. A. *J. Phys. Chem. A* **1998**, *102*, 329. (e) Hudgins D. M.; Sandford, S. A. *J. Phys. Chem. A* **1998**, *102*, 344. (f) Hudgins D. M.; Sandford, S. A. *J. Phys. Chem. A* **1998**, *102*, 353.
- (7) (a) Szczepanski, J.; Wehlberg, C.; and Vala, M. *Chem. Phys. Lett.* **1995**, *232*, 221. (b) Halasinski, T. M.; Salama, F.; Hudgins, D. M.; Allamandola, L. J. *J. Phys. Chem. A*, submitted.
- (8) Jacox, M. E. In *Reviews of Chemical Intermediates*; Strausz, O. P., Ed.; Verlag Chemie International, Inc.: New York, 1978; p 1, and references therein.
- (9) (a) Harris, S. J.; Weiner, A. M. *Combust. Sci. Technol.* **1983**, *31*, 155. (b) Frenklach, M.; Warnatz, J. *Combust. Sci. Technol.* **1987**, *51*, 265. (c) Weilmunster, P.; Keller, A.; Homann, K.-H. *Combust. Flame* **1998**, *116*, 62.
- (10) (a) *Polycyclic Hydrocarbons and Carcinogenesis*; Harvey, R. G., Ed.; American Chemical Society: Washington, D.C., 1985. (b) *Polynuclear Aromatic Hydrocarbons: Measurements, Means, and Metabolism*; Cooke, M., Loening, K., Merritt, J., Eds.; Battelle Press: Columbus, Ohio, 1991.
- (11) Milligan, D.; Jacox, M. E. *J. Phys. Chem.* **1971**, *55*, 3404.
- (12) Herbst, E.; Patterson, T. A.; Lineberger, W. C. *J. Chem. Phys.* **1974**, *61*, 1300.
- (13) Becke, A. D. *J. Chem. Phys.* **1993**, *98*, 5648.
- (14) Stephens, P. J.; Devlin, F. J.; Chabalowski, C. F.; Frisch, M. J. *J. Phys. Chem.* **1994**, *98*, 11623.
- (15) Frisch, M. J.; Pople, J. A.; Binkley, J. S. *J. Chem. Phys.* **1984**, *80*, 3265, and references therein.
- (16) Bauschlicher, C. W., Jr.; Hudgins, D. M.; Allamandola, L. J. *Theor. Chem. Acc.* **1999**, *103*, 154.
- (17) Frisch, M. J.; Trucks, G. W.; Schlegel, H. B.; Gill, P. M. W.; Johnson, B. G.; Robb, M. A.; Cheeseman, J. R.; Keith, T.; Petersson, G. A.; Montgomery, J. A.; Raghavachari, K.; Al-Laham, M. A.; Zakrzewski, V. G.; Ortiz, J. V.; Foresman, J. B.; Cioslowski, J.; Stefanov, B. B.; Nanayakkara, A.; Challacombe, M.; Peng, C. Y.; Ayala, P. Y.; Chen, W.; Wong, M. W.; Andres, J. L.; Replogle, E. S.; Gomperts, R.; Martin, R. L.; Fox, D. J.; Binkley, J. S.; Defrees, D. J.; Baker, J.; Stewart, J. P.; Head-Gordon, M.; Gonzalez, C.; Pople, J. A. *Gaussian 94*, rev. D.1; Gaussian, Inc.: Pittsburgh, PA, 1995.
- (18) Jacox, M. E. Vibrational and electronic energy levels of polyatomic transient molecules. *J. Phys. Chem. Ref. Data Monograph No. 3*; American Institute of Physics, Inc.: Woodbury, NY, 1994.
- (19) Bellamy, L. J. *The Infrared Spectra of Complex Molecules*; John Wiley and Sons: New York, 1960.
- (20) Hudgins, D. M.; Allamandola, L. J. *Ap. J. Lett.* **1999**, *516*, L41.